*R*esearch in
*A*stronomy and
*A*strophysics

Multiwavelength study of nearly face-on low surface brightness disk galaxies [*]

Dong Gao[1,2,3], Yan-Chun Liang[1,2], Shun-Fang Liu[1,2,3], Guo-Hu Zhong[1,2,3],
Xiao-Yan Chen[1,2,3], Yan-Bin Yang[1,2,4], Francois Hammer[4], Guo-Chao Yang[1,2,5],
Li-Cai Deng[1,2] and Jing-Yao Hu[1,2]

[1] National Astronomical Observatories, Chinese Academy of Sciences, Beijing 100012, China;
    ycliang@nao.cas.cn; dgao@nao.cas.cn
[2] Key Laboratory of Optical Astronomy, National Astronomical Observatories, Chinese Academy
    of Sciences, Beijing 100012, China
[3] Graduate University of Chinese Academy of Sciences, Beijing 100049, China
[4] GEPI, Observatoire de Paris-Meudon, 92195 Meudon, France
[5] Department of Physics, Hebei Normal University, Shijiazhuang 050016, China

Abstract We study the ages of a large sample (1802) of nearly face-on disk low surface brightness galaxies (LSBGs) using the evolutionary population synthesis (EPS) model PEGASE with an exponentially decreasing star formation rate to fit their multiwavelength spectral energy distributions (SEDs) from far-ultraviolet (FUV) to near-infrared (NIR). The derived ages of LSBGs are 1–5 Gyr for most of the sample no matter if constant or varying dust extinction is adopted, which are similar to most of the previous studies on smaller samples. This means that these LSBGs formed the majority of their stars quite recently. However, a small part of the sample ($\sim$2%–3%) has larger ages of 5–8 Gyr, meaning their major star forming process may have occurred earlier. At the same time, a large sample (5886) of high surface brightness galaxies (HSBGs) are selected and studied using the same method for comparisons. The derived ages are 1–5 Gyr for most of the sample (97%) as well. These results probably mean that these LSBGs have not much different star formation histories from their HSBGs counterparts. However, we should notice that the HSBGs are generally about 0.2 Gyr younger, which could mean that the HSBGs may have undergone more recent star forming activities than the LSBGs.

Key words: galaxies: evolution — galaxies: formation — galaxies: photometry — galaxies: spiral — galaxies: statistics — Ultraviolet: galaxies

1 INTRODUCTION

Low Surface Brightness Galaxies (LSBGs) were often hard to find owing to their faintness compared with the night sky, thus their properties were seldom studied and their contributions to the galaxy

population were underestimated for a long time. However, it has been suggested that LSBGs may comprise up to 1/2 of the local galaxy population (McGaugh et al. 1995).

An initial quantitative study about LSBGs was done by Freeman (1970), who noticed that the central surface brightness of 28 out of their 36 disk galaxies fell within a rather narrow range, $\mu_0(B) = 21.65 \pm 0.3$ mag arcsec^{-2}. This could be caused by selection effects (Disney 1976; Zwicky 1957). Since then, many efforts have been made to search for more LSBGs from surveys (see the reviews by Bothun et al. 1997; Impey & Bothun 1997; and the introduction part in Zhong et al. 2008). These include giant LSBGs (Sprayberry et al. 1995), red LSBGs (O'Neil et al. 1997) and the most common cases of "blue LSBGs" as late-type, disk-dominated spirals with $\mu_0(B) > 22$ mag arcsec^{-2} (Zhong et al. 2008 and the references therein). The LSBGs were generally thought to be unevolved systems with low metallicity (McGaugh 1994), low star formation rate (van der Hulst et al. 1993), a relatively high gas fraction (de Blok et al. 1996) and large amounts of dark matter (de Blok & McGaugh 1997). The age of LSBGs is also an important topic to study.

The ages of the LSBGs have long been a matter of controversy. Broadband photometric studies, complemented by Hα emission line data and synthetic stellar population modeling, predict quite a wide range for the ages of blue LSBGs: from 1–2 Gyr (Zackrisson et al. 2005) to 7–9 Gyr (Padoan et al. 1997; Jimenez et al. 1998). Ronnback & Bergvall (1994) carried out the multicolor studies of a sample of extremely blue galaxies with only small radial color gradients. In their work, BVI photometry was interpreted using spectral evolutionary models, and ages typically higher than 3 Gyr were found. Using optical/near-infrared (NIR) broadband photometry together with Hα emission line data for a subset of this sample, Zackrisson et al. (2005) found that the current observations cannot rule out the possibility that these blue LSBGs formed as recently as 1–2 Gyr ago. Schombert et al. (2001) argued on the basis of their $V - I$ colors and relative HI content that the most gas-rich LSBGs should typically have mean stellar ages below 5 Gyr. Padoan et al. (1997) and Jimenez et al. (1998) used $UBVRI$ photometry to conclude that most of the galaxies in their sample appeared to be older than about 7 Gyr. Vorobyov et al. (2009) used numerical hydrodynamic modeling to study the long-term ($\sim$13 Gyr) dynamical and chemical evolution of blue LSBGs, adopting a sporadic scenario for star formation. Their modeling strongly suggested the existence of a minimum age for blue LSBGs: 1.5–3.0 Gyr (from model $B - V$ colors and mean oxygen abundances), or 5–6 Gyr (from model Hα equivalent widths). The later value may decrease slightly if LSBGs have truncated initial mass functions (IMFs) with a smaller upper mass limit. Haberzettl et al. (2005) studied the star formation history of a sample of seven LSBGs in the HDF-S. The comparison of measured spectral energy distributions (SEDs) with the synthetic spectra extracted from the synthesis evolution model PEGASE (Fioc & Rocca-Volmerange 1997, assuming an exponentially declining star formation rate) suggested the ages of the dominant stellar populations are between 2 to 5 Gyr. This implies that the major star formation event of LSBG galaxies took place at much later stages (at $z \sim 0.2$ to 0.4).

These studies show that the ages of LSBGs are a topic for debate, and could cover a wide range, although the working sample is small in these investigations. Surely much more efforts and a much larger sample are needed for detailed studies on the ages of LSBGs. Moreover, most of these investigations are based on optical photometry which has obvious shortcomings in estimating ages of galaxies. We know that the youngest stars may dominate the ultraviolet (UV) and optical part of the spectrum, and an old stellar component will thereby be extremely difficult to detect. With the inclusion of NIR broadband photometry, one would expect to be able to constrain the ages more strictly (Bell et al. 2000; Zackrisson et al. 2005). The UV data are also needed to build SEDs of galaxies over a wider range, which will help to derive ages of galaxies more reliably. At present, the modern digital sky survey with large sky coverage provides us with a much larger sample of galaxies for doing detailed and statistical studies in many fields. Moreover, the multiwavelength data of a large set of astronomical objects from far-ultraviolet (FUV) to NIR have been carried out by highly efficient surveys and have been released for public use, such as the Galaxy Evolution Explorer (GALEX) in FUV and near-ultraviolet (NUV), the Sloan Digital Sky Survey (SDSS) in

optical and the Two Micron All Sky Survey (2MASS) in NIR. These multiwavelength data will help us to study the properties of a large sample of LSBGs. We focus on the ages of LSBGs in this work.

We will study the ages of a large sample of nearly face-on disk LSBGs selected from the SDSS Data Release 7 (DR7, Abazajian et al. 2009) main galaxy sample (MGS, Strauss et al. 2002), and then matched them with the 2MASS/NIR and GALEX/UV data, so that their SEDs could cover the range from FUV to Ks (1350 Å to 2.17 μm) bands. The size of the selected sample of LSBGs is 1802 and their $\mu_0(B) \geq 22$ mag arcsec^{-2}. Indeed, this is a follow-up work of Zhong et al. (2008) and Liang et al. (2010). In Zhong et al. (2008), we selected a large sample of LSBGs from the SDSS Data Release 4 (DR4, Adelman-McCarthy et al. 2006) main galaxy sample (Strauss et al. 2002), and presented its basic photometric properties, including correlations of disk scalelength versus B-band absolute magnitude and distance, and stellar populations from colors. In Liang et al. (2010), we studied the spectroscopic properties of this large sample of LSBGs, including dust extinction, strong emission-line ratios, metallicities and stellar mass-metallicity relations. In this work, we firstly extend the sample from DR4 to DR7, then try to obtain their multiwavelength data from FUV to Ks based on the public survey data from GALEX GR4/GR5 and the 2MASS Extended Source Catalog (XSC). Then, we use the evolutionary population synthesis (EPS) model PEGASE to fit their multiwavelength SEDs from FUV to NIR, and derive the ages of these galaxies. At the same time, a large sample of nearly face-on disk high surface brightness galaxies (HSBGs, 5886) with $\mu_0(B) < 22$ mag arcsec^{-2} is selected and the same analyses are applied for comparison.

This paper is organized as follows. In Section 2, we describe the multiwavelength observations and the selected sample. In Section 3, we describe the EPS model PEGASE, which is what we used to fit the SEDs of the galaxies, and the adopted parameters. In Section 4, we present the fitting method and the derived ages of the sample galaxies. In Section 5, the incompleteness effects are discussed. The discussions are given in Section 6. We summarize and conclude the work in Section 7. Throughout this paper, a cosmological model with H_0=70 km s^{-1} Mpc^{-1}, Ω_M=0.3 and $\Omega_\Lambda = 0.7$ has been adopted. All the magnitudes are in the AB system.

2 THE SAMPLE

Our sample galaxies are selected by matching three databases from multiwavelength surveys, i.e., the SDSS for $ugriz$ optical, 2MASS for $JHKs$ NIR, and GALEX for FUV and NUV bands.

2.1 The SDSS Sample

The SDSS[1] is the most ambitious astronomical survey ever undertaken in imaging and spectroscopy (York et al. 2000; Stoughton et al. 2002). The photometric and spectroscopic observations were conducted using the 2.5-m SDSS telescope at the Apache Point Observatory in New Mexico, USA. The imaging data were done in drift-scan mode in the five bands of $ugriz$, with effective central wavelengths of 3551, 4686, 6166, 7480 and 8932 Å, respectively (Gunn et al. 1998), and the 95% completeness limits for point sources are 22.0, 22.2, 22.2, 21.3 and 20.5 mag, respectively. The spectra are flux- and wavelength-calibrated with 4096 pixels from 3800 to 9200 Å at $R \sim$1800 (Stoughton et al. 2002).

We select 21 664 nearly face-on disk LSBGs from the SDSS-DR7 MGS by following the criteria used in Zhong et al. (2008). These are fracDev$_r < 0.25$ (indicating the fraction of luminosity contributed by the de Vaucouleurs profile relative to an exponential profile in the r-band is very small), $b/a > 0.75$ (for nearly face-on ones, a and b are the semi-major and semi-minor axes of the fitted exponential disk, respectively), $M_B < -18$ (excluding a few dwarf galaxies with this B-band absolute magnitude cutoff) and $\mu_0(B) \geq 22$ mag arcsec^{-2}. These selection criteria have also been described in Zhong et al. (2010). At the same time, 30 896 nearly face-on disk HSBGs with

---

[1] *http://www.sdss.org*

$\mu_0(B) < 22\,\mathrm{mag\,arcsec^{-2}}$ are selected for comparisons. The central surface brightnesses of our sample galaxies are calculated using the corresponding parameters provided in the SDSS catalog following the method given in Section 2.2 and equation (6) of Zhong et al. (2008). We use Petrosian magnitudes (and their errors) to represent the optical brightness of the SDSS galaxies. The Petrosian magnitudes could recover essentially all of the flux of an exponential galaxy profile (Stoughton et al. 2002), which are appropriate for our sample. All the magnitudes are converted to the AB system following Hewett et al. (2006).

2.2 The SDSS-2MASS Matched Sample

We use the 2MASS Extended Source Catalog (XSC)[2] to match the SDSS selected sample. Using the Mt. Hopkins northern 1.3-m telescope and the CTIO southern 1.3-m telescope in Chile, the 2MASS covered almost the entire sky in the J (1.25 μm), H (1.65 μm) and Ks (2.17 μm) bands, with a spatial resolution of 3″. The point-source sensitivity limits (10σ) are 15.8 (0.8 mJy), 15.1 (1.0 mJy), and 14.3 (1.4 mJy) mag in the J, H and Ks, respectively. The extended source sensitivity (10σ) is ~1 mag brighter than the point-source limits, or 14.7 (2.1 mJy), 13.9 (3.0 mJy), and 13.1 (4.1 mJy) mag at the J, H, and Ks, respectively, with the precise threshold depending on the brightness profile of the objects (Jarrett et al. 2000). The magnitude limit of typical extended sources in the Ks band is about 15.3 AB mag (Lee et al. 2010).

By matching our SDSS sample galaxies with the 2MASS XSC catalog within 3″ following Blanton et al. (2005) and Lee et al. (2010), we obtain 3523 LSBGs and 9483 HSBGs. For the J, H, and Ks, magnitudes (and their errors) of the galaxies, we adopt those from the fit extrapolation (j,h,k-m-ext) provided by the 2MASS database[3], which are assumed to better trace the galactic luminosity (Jarrett et al. 2000; Blanton et al. 2005). All the magnitudes are converted to the AB system following Blanton et al. (2005).

2.3 The SDSS-2MASS-GALEX Matched Sample

We use the GALEX (Martin et al. 2005) survey GR4/GR5[4] data to match our selected sample from SDSS and 2MASS. The GALEX was launched in 2003 April, and will cover the whole sky in the FUV (1350 – 1750 Å) and NUV (1750 – 2800 Å) bands, with spatial resolutions of 6.0″ in the FUV and 4.5″ in the NUV. The central wavelengths of FUV and NUV are 1528 Å and 2271 Å, respectively. In this paper, only the GALEX objects detected both in the NUV and FUV bands were used. The GALEX data products are made available to the general public via the MultiMission Archive at the Space Telescope Science Institute (MAST). The GALEX survey design was done for five modes, in which two of them are more related to our work, i.e., the All-sky Imaging Survey (AIS) with the goal to survey the entire sky subject to a sensitivity of $m_{AB} \sim 20.5$, and the Medium Imaging Survey (MIS), which covers 1000 deg^2 with extensive overlap of the SDSS (Martin et al. 2005; Morrissey et al. 2007).

We use the CASJobs[5] to match our SDSS-2MASS sample with the GALEX GR4/GR5 database by importing the coordinate list and then obtain their magnitudes in FUV and NUV (see the help section on the website[6]). Firstly, we import a prepared coordinate list into the database, which is for the RA and DEC of our SDSS-2MASS matched sample. Then a new table of this is created in the database. Next we search for neighbors of the objects within a radius of 5″, and then obtain a new table of GALEX-matched objects which provides the unique GALEX object identifier (objid)

---

[2] *http://www.ipac.caltech.edu/2mass/*

[3] see *http://irsa.ipac.caltech.edu/applications/Gator/*

[4] *http://galex.stsci.edu/GR4/*

[5] *http://mastweb.stsci.edu/gcasjobs/*

[6] *http://galex.stsci.edu/doc/CASJobsXTutorial.htm*

as matched_id, and also the search_id to mark which original object it corresponds to. In the case of multiple matches, we choose the nearest one with minimum matching distance. Finally, we obtain the magnitudes, fluxes and their errors for these objects. We use the GALEX product given in the "-mcat.fits" file, which is the Merged (FUV+NUV) source catalog. We adopt "nuv_mag" and "fuv_mag" (and their errors) as the magnitudes of our matched objects, which are the NUV calibrated magnitude and FUV calibrated magnitude, respectively, and "calibrated" means that values have been converted to AB magnitudes (see help in the pipeline data guide[7]).

Finally, we select 1802 LSBGs and 5886 HSBGs with FUV-to-NIR multiwavelength observations. The histogram distributions of their $\mu_0(B)$ and redshift are given in Figure 1. The median values of $\mu_0(B)$ are 22.24 mag arcsec^{-2} for LSBGs and 21.35 mag arcsec^{-2} for HSBGs (with means of 22.28 and 21.25), respectively. The corresponding median values of redshifts are 0.0732 and 0.0801 (with means of 0.0810 and 0.0886), respectively.
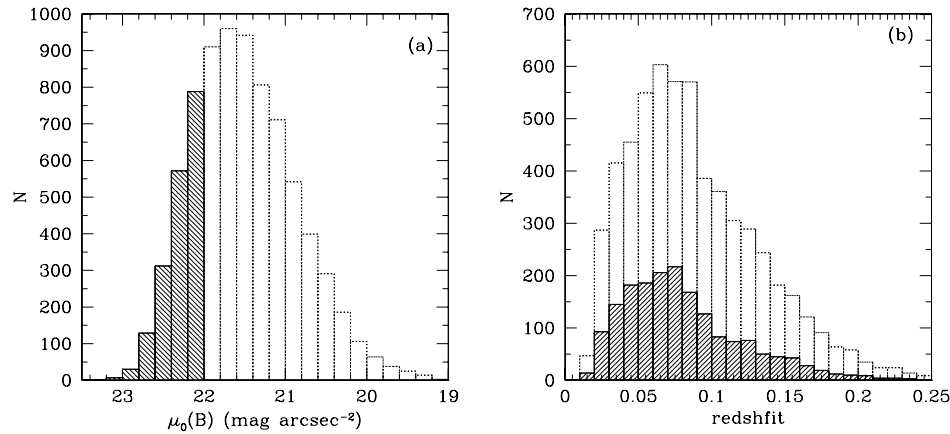

Fig. 1 Histogram distributions of $\mu_0(B)$ (with bin of 0.2) and redshift (with bin of 0.01) for our sample galaxies with FUV-to-NIR multiwavelength observations. The shaded regions refer to the LSBGs with $\mu_0(B) \geq 22$ mag arcsec^{-2}, and the dashed lines refer to the HSBGs.

2.4 Corrections of Magnitudes

The effects of foreground Galactic extinction on the observed magnitudes were calculated by using the reddening maps of Schlegel et al. (1998). The corresponding values of the SDSS and 2MASS magnitudes have been provided by Blanton et al. (2003) in the NYU-VAGC[8] catalog (thanks to them). For the GALEX FUV and NUV magnitudes, the corrections for interstellar extinctions were calculated using $A(\mathrm{FUV}) = 8.16E(B - V)$ and $A(\mathrm{NUV}) = 8.90E(B - V)$ (Rey et al. 2007; Kinman et al. 2007), and the $E(B - V)$ were taken from Schlegel et al. (1998).

The magnitudes in our sample were then corrected for redshift. We calculated the K-corrections using their K_CORRECT program, version 4.1.4, originally developed by Blanton et al. (2003) and now extended to handle GALEX data (Blanton & Roweis 2007). We corrected the observed magnitudes (FUV-to-NIR magnitudes) of the sample galaxies into the magnitudes at redshift $z = 0$. We did not consider the evolutionary correction of the magnitudes of galaxies since it would not be large

in the redshift range of our sample. We did not further consider aperture corrections for the magnitudes among the three surveys since the Petrosian magnitudes in SDSS, fit extrapolation magnitudes in 2MASS and calibrated magnitudes in GALEX have been good tracers of the total luminosities of these galaxies.

For the internal reddening of the galaxy, we input dust extinction in the PEGASE model, then obtained the model SEDs after extinction when we performed the SED fittings. As for the values of internal extinction A_V, we adopted two methods, one is constant dust extinction, i.e., $A_V = 0.6$ mag for LSBGs and $A_V = 0.8$ mag for HSBGs, and the other one assumes A_V to be a free parameter varying from 0.1 to 1.6 in the fitting procedures, which come from Liang et al. (2010) regarding the dust extinction estimates from the Balmer decrement for related samples. More information will be given in Section 4.

3 EVOLUTIONARY SYNTHESIS MODEL PEGASE

Evolutionary population synthesis is a powerful tool for interpretation of the integrated spectrophotometric observations of galaxies. The most common method for model-observation comparison of stellar population analysis in galaxies or star clusters is SED fitting, combined with either the least-squares or chi-squared minimization technique (Kong et al. 2000; Gavazzi et al. 2002; Jiang et al. 2003; Li et al. 2004a,b; Fan et al. 2006; Ma et al. 2002a,b, 2007, 2009a,b; Wang et al. 2010). There are several EPS models popularly used in astrophysical studies (see Chen et al. 2009, 2010 for references therein). We use PEGASE in this work.

PEGASE is an evolutionary spectral synthesis model for describing starbursts and evolved galaxies on the Hubble sequence. It is continuous over an exceptionally large wavelength range from 220 Å up to 5 μm. It was extended to the NIR of the atlas of synthetic spectra of Rocca-Volmerange & Guiderdoni (1988) with a revised stellar library including cold star parameters and stellar tracks extended to the thermally-pulsing regime of the asymptotic giant branch (TP-AGB) and the post-AGB phase. The synthetic stellar spectral library is taken from Kurucz (1992), and was modified by Lejeune et al. (1997) to fit the observed colors. A set of reference synthetic spectra at $z = 0$, to which the cosmological k- and evolution e- corrections for high-redshift galaxies are applied, is built from fits of observational templates (Fioc & Rocca-Volmerange 1997).

With the PEGASE code, we can compute the stellar SEDs of starbursts and evolved galaxies of the Hubble sequence at any stage of evolution, within the metallicity range $Z = 10^{-4}$ to 10^{-1}. Typical parameters of PEGASE are the star formation rate (SFR) and IMF. Assuming a standard IMF, SFR and other initial conditions, such as dust extinction, the PEGASE code will return an evolutionary history and some other important properties for a given galaxy (Li et al. 2004a,b).

In our fitting analysis, the internal dust extinctions are considered in two cases, for a constant A_V (0.6 for LSBGs and 0.8 for HSBGs) and for an A_V varying within $A_V = 0.1 - 1.6$. A zero initial metallicity of interstellar medium (ISM) is taken. We adopt the exponentially decreasing SFR (SFR$(t) \propto \mathrm{e}^{-t/\tau}$) with $\tau = 0.1 - 15$ Gyr varying in the fittings. The IMF is assumed to follow the Salpeter (1955) form, $\Phi(M) = A \times M^{-\alpha}$ with $\alpha = 2.35$, a lower cutoff of $M_\mathrm{l} = 0.1\,M_\odot$ and an upper cutoff $M_\mathrm{u} = 125\,M_\odot$ (Sawicki & Yee 1998). As a result, rest-frame modeled spectra with various star formation histories are generated by running the PEGASE code.

4 MODEL FITS AND RESULTS

We present the fitting method in Section 4.1, and the fitting results in Sections 4.2 and 4.3. Extinction affects intrinsic colors of the objects and hence accurate ages, so the photometric measurements must be dereddened before running the fitting procedure. We use two methods for considering the internal dust extinction of the galaxies in the fitting procedures with constant and varying A_V.

4.1 The Fitting Method

To estimate the ages of galaxies accurately, we add UV and NIR photometric data points to the optical data. As Ma et al. (2009b) discussed, Kaviraj et al. (2007) showed that the combination of FUV and NUV photometry with optical observations in the standard broad bands enables one to efficiently break the age-metallicity degeneracy. The optical broadband colors have the more obvious problem of age-metallicity degeneracy (Worthey 1994; MacArthur et al. 2004). Again, de Jong (1996) showed that such degeneracy can be partially broken by adding NIR photometry to optical colors, which has also been stated by Bell et al. (2000), Wu et al. (2005) and Li et al. (2007).

Our observational data consist of integrated luminosities through a given set of filters (FUV, NUV, $ugriz$, $JHKs$); thus we convolved the theoretical SEDs with these filter response curves to obtain synthetic ultraviolet, optical and NIR photometry for comparison. The synthetic magnitude in the AB magnitude system for the ith filter can be computed as

$$m_i = -2.5\log\frac{\int_\lambda F_\lambda \varphi_i(\lambda)d\lambda}{\int_\lambda \varphi_i(\lambda)d\lambda} - 48.60, \tag{1}$$

where F_λ is the theoretical SED and φ_i is the response curve of the ith filter in the set of filters that we used.

We use a χ^2 minimization test to examine which model SEDs are most comparable with the observed SEDs following

$$\chi^2 = \frac{1}{d}\sum_{i=1}^{10}\frac{[m_{\lambda_i}^{\mathrm{obs}} - m_{\lambda_i}^{\mathrm{mod}}(t)]^2}{\sigma_i^2}, \tag{2}$$

where $m_{\lambda_i}^{\mathrm{mod}}(t)$ is the integrated magnitude in the ith filter of a theoretical SED at age t, $m_{\lambda_i}^{\mathrm{obs}}(t)$ represents the observed integrated magnitude in the same filter, σ_i^2 is the observational uncertainty for the ith filter magnitude, and d is the number of degrees of freedom. We did not consider the uncertainty associated with the model itself, which should be insignificant and not affect our results much. More details about the fitting method can be referred to in Li et al. (2004a,b) and Ma et al. (2009a,b). The derived ages of our sample galaxies from such SED fitting analyses are given in the next two subsections.

4.2 Constant Dust Extinction

We adopt constant $A_V = 0.6$ mag for LSBGs and $A_V = 0.8$ mag for HSBGs in these fittings by following Liang et al. (2010). In Liang et al. (2010), we derive the A_V value for each object from their spectroscopic Balmer decrement Hα/Hβ (see their fig. 2 for histogram distributions). The median values of A_V for the four subsamples (with $\mu_0(B)$ in units of mag arcsec^{-2}: vLSBGs with 22.75–24.5, iLSBGs with 22.0–22.75, iHSBGs with 21.25–22.0, vHSBGs with <21.25) are 0.46, 0.63, 0.76, and 0.83, respectively. In our present work, most LSBGs have $\mu_0(B)$ within 22–23 mag arcsec^{-2}, thus $A_V = 0.6$ is acceptable to use as their dust extinction. Also $A_V = 0.8$ is reasonable to use as the dust extinction of HSBGs.

Figure 2 shows the resulting SED fittings (top-left panel for one example of LSBGs; top-right panel for one example of HSBGs) and the histogram distributions of the derived ages of the galaxies (in the bottom panel, the shaded region is for LSBGs and the dashed line is for HSBGs). The bottom panel shows that the ages of most of the LSBGs are 1–5 Gyr with a median (mean) value of 1.63 (1.75) Gyr. This means that the majority of their stars formed quite recently. However, about 3% of the LSBGs have larger ages, 5–8 Gyr. This small portion of the galaxies could probably form their stars at an earlier time. Similarly, the ages of most of HSBGs are 1–5 Gyr as well with a median value of 1.47 (mean of 1.59) Gyr. About 3% of them have ages as large as 5–8 Gyr. This similarity may mean that the LSBGs and HSBGs could have not much different star formation histories. This

result is consistent with the metallicity estimates of similar samples presented in Liang et al. (2010). However, we should notice the fact that the HSBGs are slightly younger than the LSBGs, $\sim 0.2\,\mathrm{Gyr}$ shown by the median (mean) ages of the samples. The median (mean) ages of the sample galaxies are presented in Table 1.
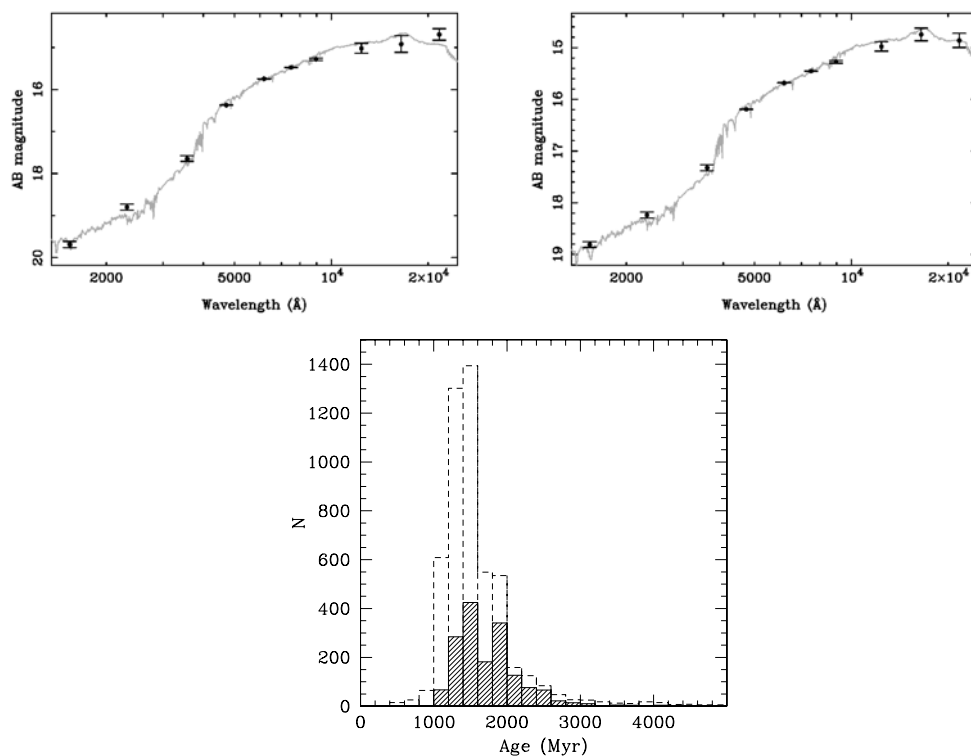

Fig. 2 Fitting results with PEGASE model and constant dust extinction ($A_V = 0.6$ for LSBGs and $A_V = 0.8$ for HSBGs) for our sample galaxies. The top-left panel shows the SED fitting for one example of LSBGs (RA $= 8.06543$, DEC $= 0.90616$ in epoch 2000, the derived age is $1.57\,\mathrm{Gyr}$), the top-right panel shows the SED fitting for one example of HSBGs (RA $= 6.75941$, DEC $= -9.63505$ in epoch 2000, the derived age is $1.44\,\mathrm{Gyr}$), and the bottom panel shows the histogram distributions of the derived ages of LSBGs (*shaded region*) and HSBGs (*dashed line*) with bin of $0.2\,\mathrm{Gyr}$.

4.3 Varying Dust Extinction

Now we vary the parameter A_V from 0.1 to 1.6 in the fittings. This range of A_V values is reasonable for LSBGs and HSBGs by following Liang et al. (2010), and 1.6 is almost the upper limit of the sample (also see Liang et al. 2007 for the SDSS star forming galaxies).

Figure 3 shows the resulting SED fittings of two example galaxies (the top-left panel for the same example of LSBGs, and the top-right panel for the same example of HSBGs as in Fig. 2) and the histogram distributions of the derived ages of the galaxies (the bottom panel, where the shaded region is for LSBGs and the dashed line is for HSBGs). The bottom panel also shows that the ages

Table 1 Derived Ages (in units of Gyr) of the Sample and Sub-sample Galaxies

	whole	volume-limited	pure disk	$r \leq 16$	pure disk + $r \leq 16$
			LSBGs		
Number	1802	1046	505	585	157
Constant A_V	1.63 (1.75)	1.60 (1.69)	1.65 (1.77)	1.54 (1.65)	1.60 (1.74)
Varying A_V	2.06 (2.18)	2.10 (2.20)	2.10 (2.20)	2.07 (2.17)	2.17 (2.30)
			HSBGs		
Number	5886	2853	1818	1553	392
Constant A_V	1.47 (1.59)	1.44 (1.53)	1.42 (1.58)	1.42 (1.53)	1.39 (1.63)
Varying A_V	1.86 (1.92)	1.90 (1.94)	1.83 (1.87)	1.93 (1.98)	1.90 (1.97)

The first part is for the LSBGs and the second part is for the HSBGs. "Number" refers to the numbers of galaxies in the sample and sub-samples. The median (mean) ages (in units of Gyr) of the galaxies are given for both the constant and varying dust extinction cases.

of most of the LSBGs are 1–5 Gyr with a median (mean) value of 2.06 (2.18) Gyr, which means that the majority of their stars were formed quite recently. However, about 2% of the LSBGs have larger ages, 5–8 Gyr, which mean that they could form their stars at earlier times. Similarly, the ages of most of the HSBGs are also 1–5 Gyr with a median value of 1.86 (mean of 1.92). About 3% of them have larger ages of 5–8 Gyr. This similarity may mean that the LSBGs and HSBGs have relatively similar star formation histories, but the HSBGs are generally 0.2 Gyr younger than the LSBGs. All these results are consistent with those obtained with constant dust extinction, although varying A_V results in a slightly older age (~ 0.4 Gyr) than the constant one. The corresponding ages are also presented in Table 1.

5 INCOMPLETENESS EFFECTS

It is important to test the completeness of the sample, and discuss its effect on the derived ages of the galaxies.

5.1 The Volume-limited Sub-sample

The incompleteness of the sample could affect the derived results of our analysis, thus it is important to test. Zhong et al. (2008) have carefully discussed the incompleteness of the sample of LSBGs. In their section 2, the good completeness of the SDSS MGS has been discussed. The MGS is a spectroscopic sample selected from the SDSS photometric data. The completeness for objects with spectroscopic observations is high, exceeding 99%, and the fraction of galaxies eliminated by the surface brightness cut is very small ($\sim 0.1\%$). Relative to all the SDSS targets, the SDSS spectroscopic survey is 90% complete (Blanton et al. 2003; Hogg et al. 2004; Strauss et al. 2002; McIntosh et al. 2006). Blanton et al. (2005) thoroughly discussed the incompleteness at low surface brightness, and presented the contributions to completeness as a function of surface brightness, the r-band Petrosian half-light surface brightness $\mu_{50,r}$. It shows that, for those brighter ones with $\mu_{50,r} < 23$ mag arcsec^{-2} (corresponding to $\mu_0(B) = 24.5$ mag arcsec^{-2}), the completeness of the spectroscopy is very close to 100%. However, for the photometric and tilling catalogs, they show obvious incompleteness within $\mu_{50,r} = 22 - 23$ mag arcsec^{-2}, so the total completeness there could decrease to about 70%.

Similar to Zhong et al. (2008) in their section 5, here we also extract a volume-limited subsample to minimize the effects of sample incompleteness on the derived ages of galaxies. We firstly extract a volume-limited sub-sample from the $M_r - z$ plane by considering $z < 0.1$ and those brighter than the corresponding M_r from the SDSS-DR7 MGS as given in Section 2.1. We obtain 5608 LSBGs and 8046 HSBGs. Then, we match them with our sample galaxies having FUV to NIR
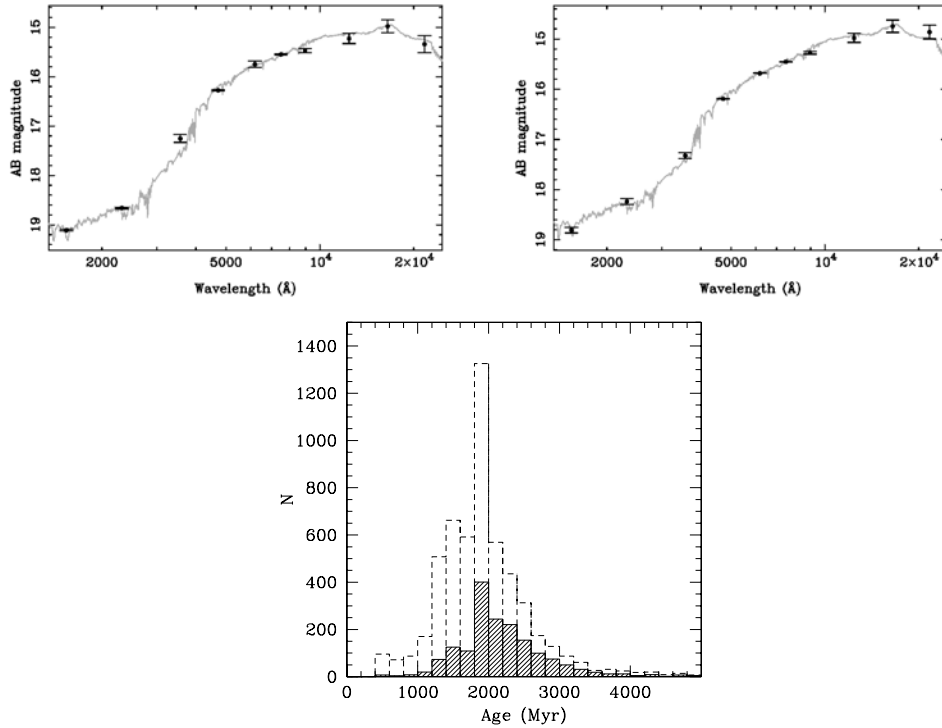
Fig. 3 Fitting results with the PEGASE model and varying dust extinction ($A_V = 0.1 - 1.6$) for our sample galaxies. The top-left panel shows the SED fitting for one example of LSBGs (same as in Fig. 2, but the derived age is 2.10 Gyr), the top-right panel shows the SED fitting for one example of the HSBGs (same as in Fig. 2 but the derived age is 1.96 Gyr), and the bottom panel shows the histogram distributions of the derived ages of LSBGs (*shaded region*) and HSBGs (*dashed line*) with a bin size of 0.2 Gyr.

SEDs (i.e., the 1802 LSBGs and 5886 HSBGs). This allows us to obtain a sub-sample including 1046 LSBGs and 2853 HSBGs. Their ages are given in Figure 4 as histogram distributions. The left panel is for the constant dust extinction, same as in Figure 2, and the right panel is for the varying dust extinction, same as in Figure 3. The left one shows that the median (mean) ages are 1.60 (1.69) Gyr for LSBGs and 1.44 (1.53) Gyr for HSBGs sub-samples. The right panel shows that the corresponding median (mean) ages are 2.10 (2.20) Gyr for LSBGs and 1.90 (1.94) Gyr for HSBGs sub-samples. These derived ages of the volume-limited sub-sample are very similar to those of the whole sample (Figs. 2 and 3) with only 0.02–0.06 Gyr discrepancies in ages. This verifies the robustness of our results. The derived ages are also presented in Table 1.

5.2 The Pure Disk Sub-sample

It is also necessary to check the effects of the calculated central surface brightness on our results. In the sample criteria (Sect. 2.1), we adopted fracDev$_r$ < 0.25 to guarantee that the disk light (in r-band) will be well explained by an exponential profile. To entirely remove the effect of bulge
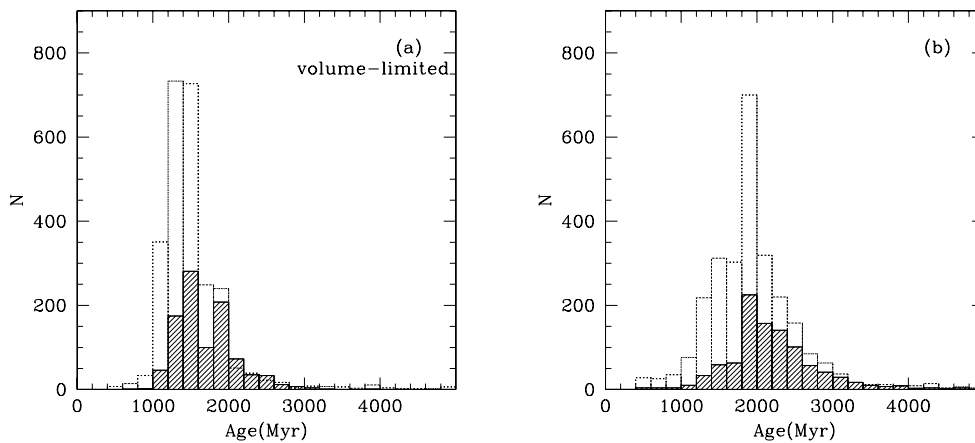
Fig. 4 Histogram distributions of ages (bin size of 0.2) of the volume-limited sub-samples of LSBGs (*shaded region*) and HSBGs (*dotted line*). The left panel is for the constant dust extinction case (see Sect. 4.2) and the right panel is for the varying dust extinction case (see Sect. 4.3).

light, we select a sub-sample of pure disks with $fracDev_r = 0$. This sub-sample includes 8453 LSBGs and 12 096 HSBGs from the SDSS-DR7 MGS. Then we match these sub-sample galaxies with our sample galaxies having FUV to NIR SEDs, so we obtain 505 LSBGs and 1818 HSBGs. The derived ages of these sub-sample galaxies are given in Figure 5. The left panel shows the results with constant dust extinction, and the median (mean) ages are 1.65 (1.77) Gyr for LSBGs and 1.42 (1.58) Gyr for HSBGs sub-samples. The right panel shows the results with varying dust extinction, and the corresponding median (mean) ages are 2.10 (2.20) Gyr for LSBG sub-samples and 1.83 (1.87) Gyr for HSBG sub-samples. These results are also very similar to the derived ages of the whole sample of LSBGs and HSBGs (given in Figs. 2 and 3), respectively, and are also similar to those from the volume-limited sub-sample (given in Fig. 4). The discrepancy is 0.02–0.08 Gyr. These results are presented in Table 1 as well.

We use criterion $fracDev_r < 0.25$ to select the disk galaxies in our work as shown in Section 2.1. To carefully check whether the central surface brightness of galaxies depends on $fracDev_r$, we obtain the relations of $\mu_0(B)$ vs. $fracDev_r$ for our LSBGs. It shows a very small slope in their least-square fitting relation, -0.08 (i.e. $\mu_0(B) = -0.08\ fracDev_r + 22.51$). This negative value does show that, for the galaxies having higher $fracDev_r$, their central surface brightness may be slightly overestimated by an exponential disk profile, however, the discrepancy is quite small. We also check this relation for HSBGs, and the corresponding slope is also small, -0.30. These verify that $fracDev_r < 0.25$ could be a reasonable criterion to select disk galaxies, and will not affect our calculations of the central surface brightnesses of galaxies much. This criterion has already been more strict than what is used in literatures; for example, Chang et al. (2006) and Shao et al. (2007) used $fracDev_r < 0.5$ to select their spiral galaxies.

5.3 The $r \leq 16$ Sub-sample

It is well known that 2MASS is shallow, so we may worry that the results obtained from 2MASS will be biased toward the massive galaxies. McIntosh et al. (2006) helpfully made a cross-correlation of the well-defined and highly complete spectroscopic selection of $r \leq 17.5$ mag galaxies in the SDSS MGS with the 2MASS sources to explore the nature and completeness of the 2MASS (K-
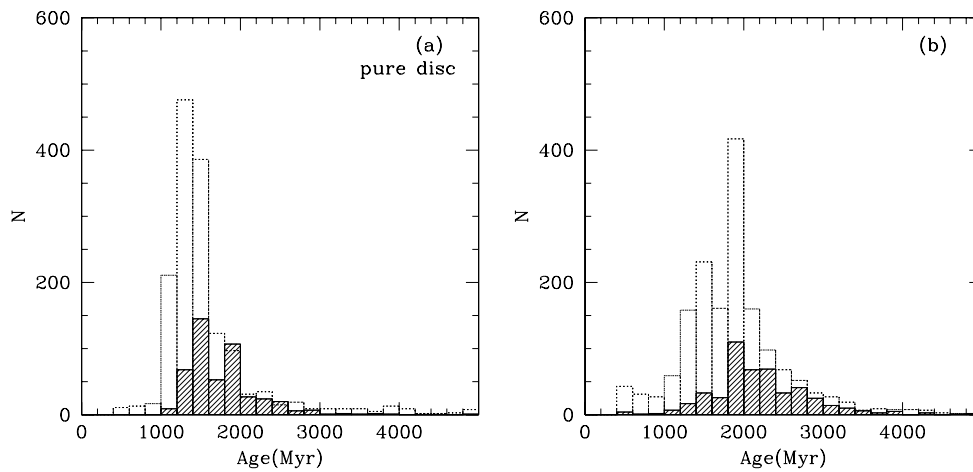
Fig. 5 Histogram distributions of ages (bin of 0.2) of the pure disk sub-samples of LSBGs (*shaded region*) and HSBGs (*dotted line*) with fracDev$_r$ = 0. The left panel is for the constant dust extinction case (see Sect. 4.2) and the right panel is for the varying dust extinction case (see Sect. 4.3).
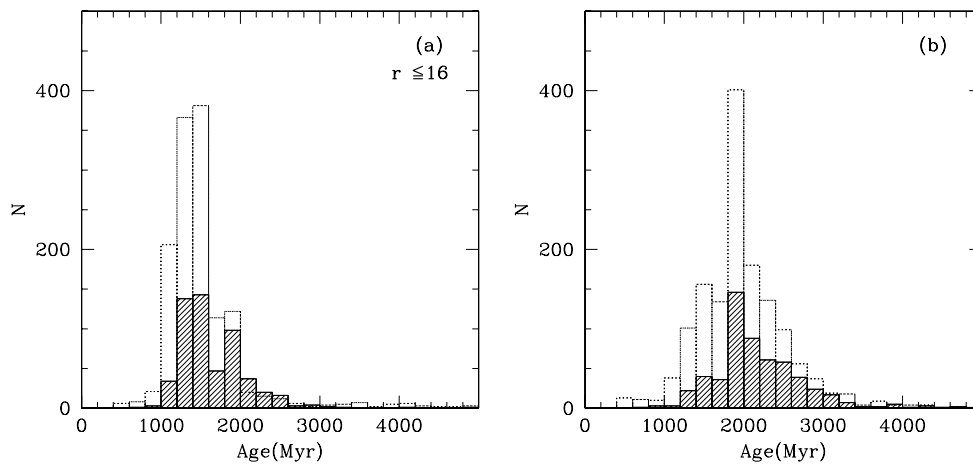

Fig. 6 Histogram distributions of ages (bin size of 0.2) of the $r \leq 16$ sub-samples of LSBGs (*shaded region*) and HSBGs (*dotted line*). The left panel is for the constant dust extinction case (see Sect. 4.2) and the right panel is for the varying dust extinction case (see Sect. 4.3).

band) selection of nearby galaxies. They quantified the completeness of 2MASS galaxies in terms of optical properties from SDSS, and found, for $r \leq 16$ mag, 94.5 per cent of the MGS is in the 2MASS XSC. An XSC completeness of 97.6 per cent is achievable at bright magnitudes, with blue low-surface-brightness galaxies being the only major source of incompleteness. They concluded that the rapid drop in XSC completeness at $r > 16$ mag reflects the sharp surface-brightness limit of the extended source detection algorithm in 2MASS. A combined $K \leq 13.57$ and $r \leq 16$ mag-limited selection provides the most representative inventory of galaxies in the local cosmos with NIR and optical measurements, which has 92.2 per cent completeness.

Therefore, we select a sub-sample with $r \leq 16$ mag from our LSBGs and HSBGs (they have $K \leq 13.57$), and then compare their derived ages with those of the whole sample. First, the galaxies with $r \leq 16$ are selected from the SDSS-DR7 MGS; this results in 1855 LSBGs and 2485 HSBGs. These galaxies are further matched with our sample galaxies having FUV to NIR SEDs, which then results in a sub-sample including 585 LSBGs and 1553 HSBGs, respectively. Their ages are given in Figure 6 as histogram distributions. The left panel shows the results with constant dust extinction, and the median (mean) ages are 1.54 (1.65) Gyr for LSBGs and 1.42 (1.53) Gyr for HSBGs sub-samples. The right panel shows the results with varying dust extinction, and the corresponding median (mean) ages are 2.07 (2.17) Gyr for LSBGs and 1.93 (1.98) Gyr for HSBGs sub-samples. These derived ages of the sub-sample are similar to those of the whole sample as given in Figures 2 and 3, and to the other two sub-samples as given in Figures 4 and 5, respectively. The discrepancy is only up to 0.12 Gyr. These results are given in Table 1.

5.4 The Pure Disk with $r \leq 16$ Sub-sample

In this subsection, we perform one more test to check the robustness of our estimates by further extracting a subsample with fracDev$_r = 0$ and $r \leq 16$ mag, i.e. the pure disks with $r \leq 16$ mag. That is, we select the sub-sample by matching the galaxies in Sections 5.2 and 5.3. This results in 161 LSBGs and 341 HSBGs. The distributions of their derived ages are presented in Figure 7.

The left panel shows the results with constant dust extinction, and the median (mean) ages are 1.60 (1.74) Gyr for LSBGs sub-samples and 1.39 (1.63) Gyr for HSBGs sub-samples. The right panel shows the results with varying dust extinction, and the corresponding median (mean) ages are 2.17 (2.30) Gyr for LSBG and 1.90 (1.97) Gyr for HSBG sub-samples. These derived ages of the sub-samples are similar to those of the whole sample as given in Figures 2 and 3, and to the other three sub-samples as given in Figures 4, 5, and 6. The discrepancy is only up to 0.13 Gyr. The results are also given in Table 1.

All the consistencies among the whole sample and the four sub-samples about the derived ages of the sample galaxies confirm well the robustness of our analyses. To be clear, all the results are summarized in Table 1.
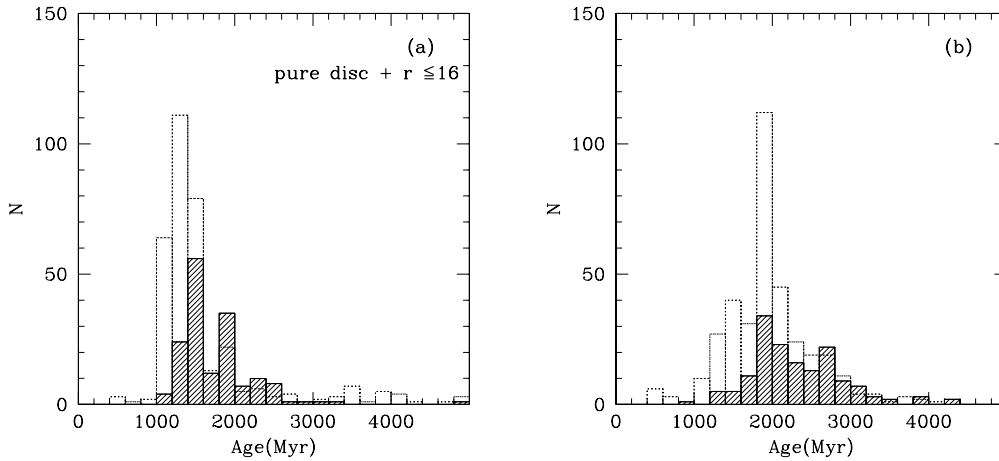

Fig. 7 Histogram distributions of ages (bin size of 0.2) for the pure disk with $r \leq 16$ sub-samples of LSBGs (*shaded region*) and HSBGs (*dotted line*). The left panel is for the constant dust extinction case and the right panel is for the varying dust extinction case.

6 DISCUSSIONS

6.1 Comparisons with Previous Studies

We study the ages of LSBGs using the EPS model PEGASE with exponentially decreasing SFR to fit their multiwavelength SEDs from FUV to NIR. The HSBGs are also applied to similar studies as comparisons. First, we find that the derived ages are 1–5 Gyr for most of our large sample of 1802 LSBGs, which is consistent with most of the previous studies based on smaller samples.

Schombert et al. (2001) studied the $V-I$ colors and relative H I content of the most gas-rich LSB dwarf galaxies. They suggested that the low stellar densities of their gas-rich LSB dwarfs are due to inefficient conversion of gas mass into stellar mass. The further comparison with star formation models (Boissier & Prantzos 2000) indicated that the blue optical colors of LSB dwarfs can only be explained by dominant stellar populations less than 5 Gyr in mean age.

Zackrisson et al. (2005) used optical/NIR broadband photometry together with Hα emission line data to study the ages of a sample of nine blue LSBGs. They found that the current observations cannot rule out the possibility that these blue LSBGs formed as recently as 1–2 Gyr ago. Indeed, their Figure 3 shows that the blue colors of the group of blue LSBGs ($B-V \sim 0.4$ mag, $V-J \sim 1.2$ mag) can be well represented by an absolute age of 3.0 Gyr, an average age of 2.2 Gyr and a star formation history with $\tau = 1.0$ Gyr. However, they also present much older possible ages, such as 13 Gyr and 7.4 Gyr. Indeed, our results here from thousands of LSBGs confirm their young age results.

In Vorobyov et al. (2009), they used numerical hydrodynamic modeling and found the existence of a minimum age for blue LSBGs: 1.5–3.0 Gyr or 5–6 Gyr. They complement hydrodynamic modeling with population synthesis modeling to produce the integrated $B-V$ colors and Hα equivalent widths. They adopted a sporadic model for star formation which yields no radial abundance gradients in the model disk (as observed by de Blok & van der Hulst 1998). They also mentioned that this sporadic star formation was in agreement with the studies showing that the current star formation of LSBGs is localized to a handful of compact regions (Auld et al. 2006 from Hα imaging), and then there is little or no diffuse Hα emission coming from the rest of the galactic disk. We may need more observations of LSBGs to further support this conclusion.

The most similar and comparable work with us is Haberzettl et al. (2005), who studied the star formation history of seven LSBGs in the HDF-S by comparing the measured SEDs with the synthetic spectra extracted from PEGASE. Comparing a library of SEDs to the measured spectra, they were able to derive ages between 2 to 5 Gyr for the dominant stellar population. All these investigations above, as well as ours with a much larger sample, favor a scenario that the major star formation events of LSBG galaxies took place at much later stages (at $z \sim 0.2$ to 0.4).

However, Padoan et al. (1997) concluded that most of the LSBGs in their sample appeared to be older than about 7 Gyr. In the work, Padoan et al. (1997) used a new IMF derived from numerical fluid dynamics simulations and a new synthetic stellar population code obtained in their earlier works. Jimenez et al. (1998) further improved their model and obtained similar results about ages of LSBGs (older than 7 Gyr). In fact, a part of our LSBGs ($\sim 2\%$–3%) also has ages as large as 5–8 Gyr, which could be consistent with Padoan et al. (1997) and Jimenez et al. (1998). These could mean that some of the LSBGs may form the majority of their stars at an earlier time.

6.2 Comparing the LSBGs and HSBGs

Another aspect of the results of this work is that the HSBGs do not show very different ages from the LSBGs. The ages of most of the HSBGs are also 1–5 Gyr with part of them (3%) having ages as large as 5–8 Gyr. This is not unlikely and consistent with some other investigations. Mattsson et al. (2007) study the chemical evolution of LSBGs. They conclude that LSBGs probably have the same ages as their high surface brightness counterparts, although the global rate of star formation must be considerably lower in these galaxies. Boissier et al. (2003) compared the observed properties with

the predictions of models of the chemical and spectrophotometric evolution of LSBGs; the basic idea behind the models is that LSBGs are similar to "classical" HSB spirals except for a larger angular momentum.

As van den Hoek et al. (2000) discussed, the presence of an old stellar population in many late-type LSBGs, as indicated by the optical colors and confirmed by their galactic chemical and photometric evolution model, suggested that LSBGs roughly follow the same evolutionary history as HSBGs, but at a much lower rate. The mean age of the stellar population in most LSBGs and HSBGs was similar, even though the disks of LSBGs were in a relatively early evolutionary stage.

Although Haberzettl et al. (2005) found that the HSBGs from Kennicutt (1992) have much larger ages than their LSBGs, in fact, their figure 2 shows that some of the objects of Kennicutt (1992) do have quite young ages < 4 Gyr, and many of the objects of Kennicutt (1992) have SEDs of early-type galaxies (E or S0), which should not be very similar to our galaxies here which are face-on disks. Similarly, the relatively high ages of the HSBGs in Terlevich & Forbes (2002) and Caldwell et al. (2003) could also be due to most of their samples being early-type galaxies.

The similar ages between LSBGs and HSBGs obtained in this work could be consistent with Liang et al. (2010) regarding the metallicity analysis of the LSBGs and HSBGs, which also comes from the parent sample of Zhong et al. (2008). They found that the LSBGs and HSBGs are located close to the stellar mass vs. metallicity and N/O vs. O/H relations of the normal galaxies, but the LSBGs have slightly higher N/O than the HSBGs at a given O/H in the low metallicity region. This may mean that the LSBGs could have relatively lower SFR than the HSBGs and then show a dominant primary nitrogen component there as Molla et al. (2006, their fig. 5) suggested. However, we should notice that the derived ages of HSBGs in this work are generally about 0.2 Gyr younger than those of the LSBGs (see Table 1). This may mean that HSBGs may have undergone their star formation process more recently than the LSBGs, or the recent star formation process is stronger in HSBGs than in LSBGs. This is also consistent with the results of Chen et al. (2010, in preparation) for the stellar population analysis of spectral absorption lines and continua of Liang et al. (2010)'s sample, in which they found that the HSBGs have a slightly larger fraction (5%) of the young population than the LSBGs. In a word, as Liang et al. (2010) concluded, the large sample shows that LSBGs span a wide range in metallicity and stellar mass, and they lie nearly on the stellar mass vs. metallicity and N/O vs. O/H relations of normal galaxies. The HSBGs show similar trends. These suggest that LSBGs and HSBGs have not had dramatically different star formation and chemical enrichment histories.

6.3 Effects of Other Parameters

We adopt the exponentially decreasing SFR in PEGASE for fitting the SEDs of the sample galaxies. The derived star formation rate decay time τ of LSBGs covers a wide range from 0.1 to 15 Gyr in both cases of constant (Sect. 4.1) and varying (Sect. 4.2) dust extinction. In the constant A_V case, the median of τ is about 0.5 Gyr and the mean is 0.57 Gyr. In the varying A_V case, the median of τ is about 0.5 Gyr and the mean is 0.62 Gyr. For the HSBGs, the derived τ values are also within 0.1–15 Gyr with a median (mean) of 0.5 Gyr (0.78 Gyr) in the constant A_V case, and a median (mean) of 0.6 Gyr (0.73 Gyr) in the varying A_V case, respectively. It is similar between LSBGs and HSBGs. These values are not unacceptable. Haberzettl et al. (2005) estimated τ to be 500 Myr (two cases), 1400 Myr (three cases), and 5000 Myr (two cases) for their seven LSBGs. Li et al. (2004a) adopted $\tau = 3$ Gyr for M81, and Li et al. (2004b) adopted $\tau = 12$ Gyr for M33 in their SED fittings by using PEGASE. Zackrisson et al. (2005) also adopted a wide range of τ values in their model (0.5–15 Gyr generally, their fig. 3).

The colors and Hα emission properties of disk and irregular galaxies have shown the general picture of their star formation history. As Kennicutt (1983) and Kennicutt et al. (1994) commented, early-type galaxies (types S0-Sb) represent systems which formed most of their gas into stars on

timescales much less than the Hubble time, while the disks of late-type systems (Sc-Im) have formed stars at roughly a constant rate since they formed. They parameterized the star formation history as an exponentially declining star formation rate: $SFR(t) = R_0 e^{-t/\tau}$, where τ was adopted as 0–15 Gyr, and the $1/\tau = 0$ case corresponds to the constant star formation case (Kennicutt 1983). As Zackrisson et al. (2005) analyzed, the short burst scenario (with star formation ending very abruptly) can be ruled out for LSBGs, since it will predict a too high EW (Hα). And in the scenarios including constant or increasing star formation rates over cosmological time scales, it still predicts a too high EW (Hα) to reach the observations. This may nonetheless be remedied if the slope of the IMF is significantly more bottom-heavy or the upper mass limit substantially lower than typically assumed.

For LSBGs, Vorobyov et al. (2009) used a simple model of sporadic star formation in which the individual star formation sites (SFSs) are distributed randomly throughout the galactic disk, which is reasonable for LSBGs. They further point out there is evidence that star formation in blue LSBGs does not proceed at a near-constant rate. Their own numerical simulations and modelling by Zackrisson et al. (2005) indicated that the SFR should be declining with time to reproduce the observed EW (Hα) in LSBGs. Therefore, they assumed an exponentially decreasing SFR in their modelling. Moreover, van den Hoek et al. (2000) found that most of the LSBGs in their sample belonged to the group of late-type galaxies for which exponentially decreasing SFR models were in good agreement with the observations. Haberzettl et al. (2005) also pointed out that the spectra of their sample galaxies were all represented by an exponentially decreasing star formation rate. Therefore, it is reasonable for us to adopt the exponentially decreasing SFR for our LSB sample galaxies by following the discussions above. We also adopt the same form of SFR for the HSBGs to be consistent. However, we have tried to use the constant SFR instead in PEGASE to fit the SEDs of all our sample galaxies. The resulting ages of galaxies become slightly larger than those with an exponentially decreasing SFR. It is generally $\sim 5 - 6$ Gyr. This could be understood from the model prediction, i.e., for the constant SFR case, it may need a longer time to assemble the equivalent amount of stellar populations.

The degeneracy between age and metallicity is often a problem in stellar population analysis of galaxies. It is not easy to degenerate them. In our fittings, we obtain the metallicity Z of galaxies from 0.0001 to 0.04 covering a wide range for most of the sample galaxies. As far as we know, the metallicity presented by PEGASE is the value averaged over the Simple Stellar Populations (SSPs) with various metallicities, and the average is sensitive to the dominant populations among all the SSPs. Moreover, by adding UV and NIR photometric data to the optical data, the degeneracy between age and metallicity could be efficiently broken as discussed in Section 4.1. Thus, the dominate stellar population ages derived here from PEGASE with SED fittings should be robust.

The derived ages of galaxies discussed here represent the time-scale since their dominant stellar populations formed. This could be different from the stellar mean ages of the galaxies. The PEGASE model also provides the mean ages of the stars averaged over the bolometric luminosity. We check their values by following the items in Table 1, and found that these mean ages of stars are generally about 0.9 Gyr younger. This could be understood from the model prediction since the stars are assumed to form later than the time corresponding to the ages of galaxies.

7 CONCLUSIONS

We summarize and conclude our work in these four items:

(1) A much larger sample (1802) of nearly face-on disk LSBGs are studied in terms of their ages by fitting their multiwavelength SEDs from FUV to NIR using the EPS model PEGASE. The exponentially decreasing SFR is adopted. The ages of LSBGs cover a wide range. Most of them generally have ages of 1–5 Gyr no matter if the constant or varying dust extinction A_V are considered (the varying dust extinction results in ~ 0.4 Gyr older ages than the constant one). This age range is consistent with most of the previous studies on a smaller sample of LSBGs.

In addition, a part of the LSBGs ($\sim$2%–3%) have ages as large as 5–8 Gyr. These derived ages are also consistent with some earlier works. We should notice that if a constant SFR is adopted instead, the derived ages of sample galaxies will become slightly larger, generally $\sim$5–6 Gyr, which acts as a further check although it has been commented that the exponentially decreasing SFR is favored for LSBGs.

(2) A large sample (5886) of nearly face-on disk HSBGs is also selected and studied using the same procedure for comparisons. The results show that most of these HSBGs also have ages 1–5 Gyr, but with $\sim$3% having ages as large as 5–8 Gyr, which are not much different from the LSBGs. However, the HSBGs are about 0.2 Gyr younger than the LSBGs, which may indicate that the HSBGs have more recent star forming activities than the LSBGs.

(3) Four sub-samples are further selected for checking the incompleteness effects: the volume-limited one selected from the $M_r - z$ plane ($z < 0.1$ and those brighter than the corresponding M_r), the pure disk one with fracDev$_r = 0$, the $r \leq 16$ one for testing 2MASS completeness, and further the pure disk with $r \leq 16$ one. All the four sub-samples show quite similar results to the whole sample, i.e., the derived ages of the sample galaxies are quite similar to each other, and only have a small discrepancy, 0.02–0.13 Gyr.

(4) The similar ages between LSBGs and HSBGs could be consistent with their metallicity and stellar population analysis (Liang et al. 2010; Chen et al. 2010, in preparation). These suggest that LSBGs and HSBGs have not had dramatically different star formation and chemical enrichment histories.

References

Abazajian, K. N., et al. 2009, ApJS, 182, 543
Adelman-McCarthy, J. K., et al. 2006, ApJS, 162, 38
Auld, R., de Blok, W. J. G., Bell, E., & Davies, J. I. 2006, MNRAS, 366, 1475
Bell, E. F., Barnaby, D., Bower, R. G., et al. 2000, MNRAS, 312, 470
Blanton, M. R., et al. 2003, AJ, 125, 2348
Blanton, M. R., et al. 2005, AJ, 129, 2562
Blanton, M. R., & Roweis, S. 2007, AJ, 133, 734
Boissier, S., et al. 2003, MNRAS, 343, 653
Boissier, S., & Prantzos, N. 2000, MNRAS, 312, 398
Bothun, G. D., Impey, C., & McGaugh, S. 1997, PASP, 109, 745
Caldwell, N., Rose, J. A., & Concannon, K. D. 2003, AJ, 125, 2891
Chang, R. X., Shen, S. Y., Hou, J. L., Shu, C. G., & Shao, Z. Y. 2006, MNRAS, 372, 199
Chen, X. Y., Liang, Y. C., Hammer, F., et al. 2009, A&A, 495, 457
Chen, X. Y., Liang, Y. C., Hammer, F., et al. 2010, A&A, 515, A101
de Blok, W. J. G., McGaugh, S. S., & van der Hulst, J. M. 1996, MNRAS 283, 18

de Blok, W. J. G., & McGaugh, S. S. 1997, MNRAS, 290, 533

de Blok, W. J. G., & van der Hulst, J. M. 1998, A&A, 335, 421

de Jong, R. S. 1996, A&A, 313, 377

Disney, M. J. 1976, Nature, 263, 573

Fan, Z., Ma, J., de Grijs, R., et al. 2006, MNRAS, 371, 1648

Fioc, M., & Rocca-Volmerange, B. 1997, A&A, 326, 950

Freeman, K. C., 1970, ApJ, 160, 811

Gavazzi, G., et al. 2002, ApJ, 576, 135

Gunn, J. E., et al. 1998, AJ, 116, 3040

Haberzettl, L., Bomans, D. J., & Dettmar, R.-J. 2005, in AIP Conf. Ser. 783, The Evolution of Starbursts, 296

Hewett, P. C., Warren, S. J., Leggett, S. K., & Hodgkin, S. T. 2006, MNRAS, 367, 454

Hogg, D. W., et al. 2004, ApJ, 601, L29

Impey, C. D., & Bothun, G. D. 1997, ARA&A, 35, 267

Jarrett, T. H., Chester, T., Cutri, R., Schneider, S., Skrutskie, M., & Huchra, J. P. 2000, AJ, 119, 2498

Jiang, L., Ma, J., Zhou, X., Chen, J., Wu, H., & Jiang, Z. 2003, AJ, 125, 727

Jimenez, R., Padoan, P., Matteucci, F., & Heavens, A. F. 1998, MNRAS, 299, 123

Kaviraj, S., Rey, S.-C., Rich, R. M., Yoon, S.-J., & Yi, S. K. 2007, MNRAS, 381, L74

Kennicutt, R. C., Jr. 1983, ApJ, 272, 54

Kennicutt, R. C., Jr. 1992, ApJ, 388, 310

Kennicutt, R. C., Jr., Tamblyn, P., & Congdon, C. E. 1994, ApJ, 435, 22

Kinman, T. D., Salim, S., & Clewley, L. 2007, ApJ, 662, L111

Kong, X., et al. 2000, AJ, 119, 2745

Kurucz, R. L. 1992, in IAU Symp. 149, The stellar populations of galaxies, eds. B. Barbuy, & A. Renzini
    (Dordrecht: Kluwer Academic Publishers), 225

Lee, J. H., Lee, M. G., Park, C., & Choi, Y. Y. 2010, MNRAS, 401, 1804

Lejeune, Th., Cuisinier, F., & Buser, R. 1997, A&AS, 125, 229

Li, J. L., Zhou, X., Ma, J., & Chen, J. S. 2004a, ChJAA (Chin. J. Astron. Astrophys.), 4, 143

Li, J., Ma, J., Zhou, X., Jiang, Z., Yang, Y., & Chen, J. 2004b, A&A, 420, 89

Li, Z., Han, Z., & Zhang, F. 2007, A&A, 464, 853

Liang, Y. C., Hammer, F., Yin, S. Y., et al. 2007, A&A, 473, 411

Liang, Y. C., Zhong, G. H., Hammer, F., et al. 2010, MNRAS, in press, arXiv: 1004.3683

Ma, J., Zhou, X., Chen, J. S., et al. 2002a, A&A, 385, 404

Ma, J., Zhou, X., Chen, J. S., et al. 2002b, AJ, 123, 3141

Ma, J., Yang, Y. B. Burstein, D., et al. 2007, ApJ, 659, 359

Ma, J., de Grijs, R., Fan, Z., et al. 2009a, RAA, 9, 641

Ma, J., Fan, Z., de Grijs, R., et al. 2009b, AJ, 137, 4884

MacArthur, L. A., Courteau, S., Bell, E., & Holtzman, J. A. 2004, ApJS, 152, 175

Martin, D. C., et al. 2005, ApJ, 619, L1

Mattsson, L., Caldwell, B., & Bergvall, N. 2008, in ASP Conf. Ser. Vol. 396, Formation and Evolution of Galaxy
    Disks, eds. J. G. Funes, & E. M. Corsini (San Francisco: Astronomical Society of the Pacific), 155

McGaugh, S. S. 1994, ApJ, 426, 135

McGaugh, S. S., Schombert, J. M., & Bothun, G. D. 1995, AJ, 109, 2019

McIntosh, D. H., Bell, E. F., Weinberg, M. D., & Katz, N. 2006, MNRAS, 373, 1321

Molla, M., Vilchez, J. M., Gavilan, M., & Diaz, A. I. 2006, MNRAS, 372, 1069

Morrissey, P., et al. 2007, ApJS, 173, 682

O'Neil, K., Bothun, G. D., Schombert, J., Cornell, M. E., & Impey, C. D. 1997, AJ, 114, 2448

Padoan, P., Jimenez, R., & Antonuccio-Delogu, V. 1997, ApJ, 481, L27

Rey, S. -C., et al. 2007, ApJS, 173, 643

Rocca-Volmerange B., & Guiderdoni B. 1988, A&AS 75, 93

Ronnback, J., & Bergvall, N. 1994, A&AS 108, 193

Salpeter, E. E. 1955, ApJ, 121, 161

Sawicki, M., & Yee, H. K. C. 1998, AJ, 115, 1329

Schlegel, D. J., Finkbeiner, D. P., & Davis, M. 1998, ApJ, 500, 525

Schombert, J. M., McCaugh, S. S., & Eder, J. A. 2001, AJ, 121, 2420

Shao, Z. Y., Xiao, Q. B., Shen, S. Y., Mo, H.J., Xia, X. Y., & Deng, Z. G. 2007, ApJ, 659, 1159

Sprayberry, D., Impey, C. D., Bothun, G. D., & Irwin, M. J. 1995, AJ, 109, 558

Stoughton, C., et al. 2002, AJ, 123, 485

Strauss, M., et al. 2002, AJ, 124, 1810

Terlevich, A. I., & Forbes, D. A. 2002, MNRAS, 330, 547

van den Hoek, L. B., de Blok, W. J. G., van der Hulst, J. M., & de Jong, T. 2000, A&A 357, 397

van der Hulst, J. M., Skillman, E. D., Smith, T. R., et al. 1993, AJ, 106, 548

Vorobyov, E. I., Shchekinov, Y., Bizyaev, D., Bomans, D., & Dettmar, R. -J. 2009, A&A, 505, 483

Wang, S., Fan, Z., Ma, J., et al. 2010, AJ, 139, 1438

Worthey, G. 1994, ApJS, 95, 107

Wu, H., Shao, Z. Y., Mo, H. J., Xia, X. Y., & Deng, Z. G. 2005, ApJ, 622, 244

York, D., et al. 2000, AJ, 120, 1579

Zackrisson, E., Bergvall, N., & Ostlin, G. 2005, A&A, 435, 29

Zhong, G. H., Liang, Y. C., Liu, F. S., et al. 2008, MNRAS, 391, 986

Zhong, G. H., Liang, Y. C., Hammer, F., Chen, X. Y., Deng, L. C., & Flores, H. 2010, A&A, 520, A69

Zwicky, F, 1957, in Morphological Astronomy (New York: Springer-Verlag)